Polymer Chemistry

PAPER

View Article Online
View Journal | View Issue

Cite this: *Polym. Chem.*, 2014, **5**, 1372

Homogeneous near-infrared emissive polymeric nanoparticles based on amphiphilic diblock copolymers with perylene diimide and PEG pendants: self-assembly behavior and cellular imaging application

Zhen Yang,[a] Yan Yuan,[a] Rongcui Jiang,[a] Nina Fu,[a] Xiaomei Lu,[ab] Congcong Tian,[a] Wenbo Hu,[a] Quli Fan*[a] and Wei Huang*[ab]

Received 1st September 2013
Accepted 17th October 2013

DOI: 10.1039/c3py01197f

www.rsc.org/polymers

An amphiphilic diblock copolymer, poly(perylene diimide acrylate)-*block*-poly(poly(ethyleneglycol) methacrylate) (PPDA-*b*-P(PEGMA)), has been synthesized *via* the reversible addition fragmentation transfer polymerization (RAFT) method. The polymer shows self-assembly behavior in water due to the synergistic effects of the strong hydrophobic interactions and π–π stacking of perylene diimide (PDI) groups. Homogeneous polymer nanoparticles (PNPs) in aqueous solution with good water solubility and stability were formed with an average size of 64.3 ± 3.3 nm, revealed by dynamic light scattering (DLS). The PNPs showed near-infrared (NIR) emission at 660 nm instead of the traditional emission of individual PDI groups at 530 nm. The aggregation-enhanced π–π stacking and the resulting NIR emission of the PDI groups were demonstrated by spectroscopy and ^{1}H-NMR characterization. Cellular imaging of human pancreatic cancer cells was conducted with the obtained PNPs. Confocal microscopy results showed that the PNPs were located specifically within the cell cytoplasm. This study provides a new design concept to take full advantage of polymer amphipathy to fabricate nanoparticles with NIR emission for applications in bio-imaging.

1. Introduction

Bio-imaging techniques, especially fluorescence imaging, have been successfully utilized in clinical applications in recent decades.[1–3] In such applications, the optical probe is one of the most commonly used techniques because of its advantages of water solubility, low cytotoxicity, biocompatibility and near-infrared (NIR, 650–900 nm) absorption and emission, which exhibits deep tissue penetration and low autofluorescence background in biological media, and is less harmful to cells and tissues in comparison with ultraviolet (UV) light.[4] Inorganic and organic materials have been widely used in NIR fluorescent dyes. It is easier for inorganic fluorescent agents such as quantum dots (QDs) and upconversion nanoparticles (UCNPs) to achieve NIR emission and absorption.[5,6] However, the potential toxicity due to accumulation in the livers of animals and some other side effects have to be addressed and mitigated before they could be successfully used for *in vivo* imaging applications, placing great restrictions on the utilization of inorganic fluorescent agents.[7,8] Although a variety of organic dyes have been widely used as optical molecular probes,[9–11] they also have disadvantages, such as high cost and easy photobleaching. Therefore, the development of materials with good photochemical stabilities, water solubility, biocompatibity, and low price has become a hot research topic.

Recently, perylene-3,4,9,10-tetracarboxylic diimides (PDIs), with the advantages of exceptional chemical, thermal and photochemical stabilities and extremely low price, have recently found prominence in various applications, including organic solar cells,[12] biological sensors[13] and field effect transistors.[14] Also, PDIs have been extensively studied as pigment colorants for optical probes in biological imaging. However, PDIs exhibit poor solubility and visible fluorescence in water, which dramatically restrict its application as an efficient NIR fluorescent probe. To overcome the poor solubility, water soluble PDI derivatives have been obtained by introducing ionic groups, polyglycerol (PG) dendrons and poly(ethyleneglycol) methacrylate (PEGMA) through atom transfer radical polymerization (ATRP) on the perylene core or at the imide positions.[15–17] For example, Gao and coworkers reported that introducing

[a]*Key Laboratory for Organic Electronics & Information Displays and Institute of Advanced Materials, Nanjing University of Posts & Telecommunications, Nanjing 210046, China. E-mail: iamqlfan@njupt.edu.cn; Fax: +86 25 8586 6533; Tel: +86 25 8586 6396*

[b]*Jiangsu–Singapore Joint Research Center for Organic/Bio-Electronics & Information Displays and Institute of Advanced Materials, Nanjing University of Technology, Nanjing 211816, China. E-mail: wei-huang@njupt.edu.cn; Fax: +86 25 5813 9988; Tel: +86 25 5813 9001*

polyethylene glycol chains as the dendron substituent endowed PDIs with good water solubility, photostability, and low cytotoxicity.[18] Wang *et al.* prepared a well-defined polymer brush *via* ATRP by modifing PDIs with biocompatible poly(poly(ethyleneglycol)methacrylate) P(PEGMA) and used it for cell labeling.[19] However, these monodispersed PDIs only exhibited visible fluorescence, and few water-soluble PDIs probes show NIR emission, as is seen in the review by Würthner *et al.* on molecular assemblies of PDIs in water.[20]

In order to achieve NIR emission, Swager *et al.* extended the π-conjugation by going from PDIs to hexarylenediimides, leading to a gradual bathochromic shift of the emission maximum.[21] However, the synthesis of the increased degree of annulation is relatively complicated, and difficult to realize water solubility. Recent studies have found that the π–π stacking induced aggregation among PDIs can also effectively lead to a red-shift of the fluorescence. Li *et al.* designed a perylene-derivative molecule presenting a dynamic self-organization phenomenon driven by π–π molecular orbital overlap, which induced a fluorescence red-shift.[22] Thelakkat and co-workers reported that the emission color of the solution red-shifted from orange to NIR when increasing the number of repeat units of perylene diimide acrylate (PDA, a PDI derivative) in poly(perylene diimide acrylate) (PPDA).[23] Unfortunately, although the appropriate aggregation of PDIs can realize NIR emission, it also reduces the water solubility of PDIs.

We herein report PPDA-*block*-P(PEGMA) (PPDA-*b*-P(PEGMA)) diblock copolymers which can simply combine NIR fluorescence emission, good water solublity and biocompatibility through their self-assembly into polymeric nanoparticles (PNPs) in aqueous solution. These uniform diblock copolymers were synthesized through reversible addition fragmentation transfer polymerization (RAFT).[24] As we know, PEGMA (a PEG derivative) provides not only good water solubility but also good biocompatibility to these PNPs.[25] The amphiphilic diblock copolymers composed of hydrophobic and hydrophilic segments are prone to self-assemble into nanoparticles through hydrophobic interactions in aqueous solution.[26] In our system, the amphiphilic PPDA-*b*-P(PEGMA) was designed to self-assemble into nanoparticles in water and induce the formation of strong π–π stacking of the hydrophobic PDA rigid units to realize the NIR emission. Furthermore, the formed water soluble nanoparticles have an average size of 60 nm, which is anticipated to be appropriate for future tumor imaging through the enhanced permeability and retention (EPR) effect (<100 nm).[27] Moreover, live cell imaging based on the PNPs was investigated and it was found that the PNPs can be efficiently internalized by PANC-1 cells and accumulated in the cytoplasm. Based on this study, it is anticipated that NIR-emission nanoparticles based on other functional PDIs can be conveniently achieved though the self-assembly of diblock copolymers, and tailored for other applications.

2. Experimental section

Materials

All chemical reagents used were purchased from Sigma-Aldrich, Alfa and TCI and were used as received. Tetrahydrofuran (THF) was distilled from sodium in the presence of benzophenone. Other organic solvents were used without further treatment. All reactions were performed under a nitrogen atmosphere. Human pancreatic cancer cells (PANC-1) were purchased from ATCC. RPMI-1640 medium, Dulbecco's modified Eagle's medium (DMEM), fetal bovine serum, L-glutamine, penicillin, 3-[4,5-dimethylthiazol-2-yl]-2,5-diphenyltetrazolium bromide (MTT reagent), Triton X-100 and streptomycin were purchased from Sigma.

Preparation of homopolymers PPDA *via* RAFT

The polymerization was performed by a reported approach with some optimizations.[28] 3-Benzylsulfanylthiocarbonylsufanylpropionic acid (X) was used as the RAFT agent.[29] A mixture of X (2.72 mg, 0.01 mmol), AIBN (0.25 mg, 0.005 mmol), PDA (200 mg, 0.246 mmol) and THF (1.5 mL) was degassed in a Schlenk tube with three freeze–pump–thaw cycles. Then the mixture was sealed under vacuum and heated at 70 °C for 8 h. The reaction mixture was then precipitated in a large excess of hexane. The polymer was collected by filtration and purified by extraction with acetone in a Soxhlet extractor. The molecular weight was characterized by GPC (M_n = 4680 g mol^{-1}, M_w/M_n = 1.21). ^{1}H-NMR (400 MHz, $CDCl_3$, δ): 8.50–7.00 ppm (br, 8H), 4.99 ppm (br, 1H), 4.50 –3.70 ppm (br, 4H), 2.40–1.10 ppm (br, 40H), 0.84 ppm (br, 6H).

Preparation of PPDA-*b*-P(PEGMA) *via* RAFT

A mixture of PPDA-X (81 mg), PEGMA (200 mg, 0.21 mmol), AIBN (0.25 mg, 0.005 mmol), and THF (1.5 mL) was degassed in a Schlenk tube with three freeze–pump–thaw cycles. The mixture was sealed under vacuum and heated at 70 °C for 8 h. The reaction mixture was precipitated in a large excess of diethyl ether and the resulting polymer was isolated by filtration. The product was further purified by dialysis in water for 48 h. The pure PPDA-*b*-P(PEGMA) copolymer was recovered after freeze-drying. The molecular weight determined by GPC (Fig. 1) was 9900 g mol^{-1}, with a moderate polydispersity of 1.32.

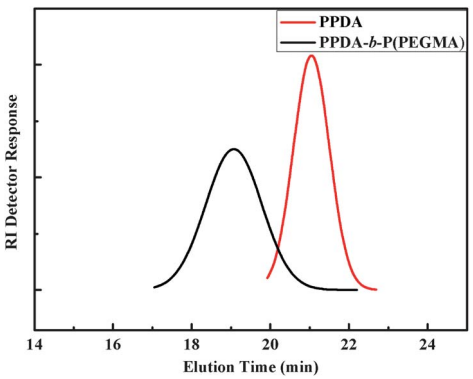

Fig. 1 GPC profiles of the PPDA-*b*-P(PEGMA) copolymer and PPDA homopolymer.

Preparation of PPDA-*b*-P(PEGMA) nanoparticles

The PNPs (1 mg mL^{-1}) were synthesized by directly adding PPDA-*b*-P(PEGMA) copolymers (5 mg) into 5 mL water in an ultrasonic apparatus for about 5 min at room temperature.

Characterization

^{1}H-NMR spectra were recorded at 20 °C on a 400 MHz NMR spectrometer (Bruker). Chemical shifts were reported in ppm using $CDCl_3$ as the solvent and tetramethylsilane as an internal standard, unless indicated otherwise. Molecular weights and polydispersities of the polymers were determined by gel permeation chromatography (GPC) analysis with polystyrene as the standard. The mobile phase was THF, flowing at 1.0 mL min^{-1}. UV-visible absorption spectra were obtained on a Shimadzu UV-3150 spectrophotometer. The PL spectra were recorded on a Shimadzu RF-5301 PC fluorometer at room temperature. Transmission electron microscopy (TEM) images were recorded on a HT7700 transmission electron microscope at an accelerating voltage of 100 kV. The TEM specimens were made by placing a drop of an aqueous solution of the nanoparticles on an ultrathin carbon-coated copper grid. The morphologies of the nanospheres were obtained on a field emission scanning electron microscope (FESEM, Hitachi S-4800). The hydrodynamic size of the copolymer nanoparticles was determined by dynamic light scattering (DLS) using a 90 Plus particle size analyzer (Brookhaven Instruments).

The cytotoxicity of the PNPs was evaluated by determining the viability of PANC-1 cells after incubation with DMEM (supplemented with 10% fetal bovine serum, 1 mM L-glutamine, 100 IU mL^{-1} penicillin) containing the PNPs at concentrations of 0.5, 0.1, 0.01, 0.001 and 0.0001 mg mL^{-1}. Cell viability testing was carried out *via* the reduction of the MTT reagent (3-[4,5-dimethylthiazol-2-yl]-2,5-diphenyltetrazolium bromide, Sigma). The MTT assay was performed in a 96-well plate following the standard procedure with minor modifications. The nanoparticles were sterilized with UV irradiation for 30 min before use. Control experiments were carried out using the complete growth culture media only (nontoxic control), and with 1% Triton X-100 (Sigma) (toxic control). PANC-1 cells were seeded at a density of 10^4 cells per well for 24 h before the medium was replaced with one containing the PNPs at concentrations of 0.1, 0.05, 0.01, 0.001 and 0.0001 mg mL^{-1}. The PANC-1 cells were incubated at 37 °C and 5% CO_2 for 24 h. The culture media from each well was then removed and 180 μL of medium and 20 μL MTT solution (5 mg mL^{-1} in PBS) were then added to each well. After 2 h of incubation at 37 °C and 5% CO_2, the media were removed and the formazan crystals were solubilized with 200 μL DMSO for 15 min. The optical absorbance was then measured at 560 nm on a microplate reader (Tecan GENios). The results were expressed as percentages relative to the results obtained with the nontoxic control. The differences in the results obtained from the PNPs and the controls were analyzed statistically using a two-sample *t*-test. The differences observed between samples were considered significant at $P < 0.05$.

The cellular imaging application of PNPs was performed using human pancreatic cancer cells (PANC-1). The cells were routinely cultured as mentioned in MTT assay section. The cultured cells were washed with PBS and detached with trypsin–EDTA solution. The cells were then collected by centrifugation and redispersed in a medium containing PNPs at a concentration of 0.01 mg mL^{-1} to achieve a cell concentration of 10^5 cells mL^{-1}. The cells were then seeded in 24-well culture plates with a chambered cover glass. Cells were washed four times after incubation for 24 h with PBS to remove the nanoparticles in the medium and then fixed by 75% ethanol for 15 min. The cell monolayer was washed twice with PBS and mounted in Dakos fluorescent mounting medium (Dako, CA) to be observed by a confocal laser scanning microscope (CLSM) (Zeiss LSM 410) with imaging software (Fluoview FV500).

3. Results and discussion

3.1. Monomers and polymers

The PDA monomer was synthesized according to the method reported by Emrick *et al.*,[30] which was confirmed by ^{1}H-NMR and GC-MS. The PPDA-*b*-P(PEGMA) copolymer was prepared by two sequential steps of the RAFT polymerization, which is shown in Scheme 1. 3-Benzylsulfanylthiocarbonylsufanylpropionic acid was chosen as a chain transfer reagent, and reacted with PDA using AIBN as an initiator. The number-average molecular weight and polydispersity of PPDA are 4680 g mol^{-1} and 1.21, respectively, measured by GPC using THF as the eluent and polystyrene as the standard. RAFT of PPDA with PEGMA was performed in THF at 70 °C for 8 h using AIBN as an initiator. The reaction mixture was precipitated in a large excess of diethyl ether to remove the unreacted PEGMA monomer, yielding PPDA-*b*-P(PEGMA) as light red fibers. Further purification by dialysis against deionized water using a 5.0 kDa molecular weight cutoff dialysis membrane for 2 days and removal of the solvent by freeze-drying left a red oily solid. The polydispersities and molecular weights of these copolymers were determined by GPC. Fig. 1 illustrates the GPC profile of the copolymers, and also the macroinitiator PPDA for comparison. The different elution times and symmetric single peaks of the homopolymer PPDA and the copolymer PPDA-*b*-P(PEGMA) indicated that the RAFT was performed well, and their low polydispersities of 1.21 and 1.32 respectively demonstrated that the desired polymer components were achieved.

The components of PPDA-*b*-P(PEGMA) were differentiated by ^{1}H-NMR in $CDCl_3$, as shown in Fig. 2. The chemical shifts at 3.26

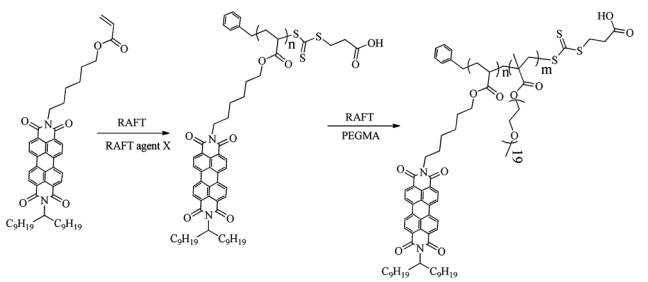

Scheme 1 Synthesis of PPDA-*b*-P(PEGMA).

ppm and 3.54 ppm (a) can be assigned to the protons of methoxyl (–OCH_3) and methylene (–OCH_2CH_2–) groups of PEGMA. The signal at 4.1 ppm (g, g′) can be assigned to methylene protons next to the ester moiety (–CH_2–OCO–) in the pendant PEGMA and PDA and the acylamino moiety (–CH_2–NCO–) in perylene. The signal at 5.1 ppm (f) can be assigned to tertiary butyl protons next to the acylamino moiety (–CH_2–NCO–) of PDA. A mass of broad peaks at around 1.0 ppm (b, c, d and h) are assigned to the methyl (–CH_3) and methylene (–CH_2–) groups of the PPDA-*b*-P(PEGMA) backbone.[31] The signal at around 8.2 ppm (e) is due to the contributions from the aromatic structure of PDA. Specific identification and integration of the end group protons was not possible from the ^{1}H-NMR spectra of the diblock copolymers. This makes it difficult to obtain the exact block lengths. However, approximate ratios of the two blocks can be obtained by integrating regions of the spectra. Because the molar ratio of the PDA and PEGMA components is about 1 : 1, calculated from the integration of bands (a), (e), (f), (g), and (g′), the molecular weight of PPDA-*b*-P(PEGMA) is determined to be 10 800, which is similar to the value from GPC (M_n = 9900) (Fig. 1). Thus, the molecular weights of PDA and PEGMA in the polymer are 4680 and 5220 g mol^{-1} respectively, from which it can be calculated that there are 6 repeat units of PDA and 6 repeat units of PEGMA in one polymer chain. We initially synthesized PPDA-*b*-P(PEGMA) with the component ratio 2 : 1, which had poor solubility in water, while a 1 : 1 ratio of PDA to PEGMA resulted in copolymers with good solubility. So, we speculate that increased water solubility can be achieved by increasing the polymerization degree of PEGMA.

The structure of PPDA-*b*-P(PEGMA) can also be demonstrated by FT-IR. The FT-IR spectrum of the PPDA homopolymer is compared with that of PPDA-*b*-P(PEGMA) copolymer in Fig. 3. The appearance of the peak at 1113 cm^{-1} (C–O stretching) belonging to PEGMA for the PPDA-*b*-P(PEGMA) provides strong evidence to prove the successful functionalization of the end of PPDA chain with PEGMA.

The controlled RAFT polymerization we used is an outstanding method for producing polymers because of the relatively mild reaction conditions and exceptional control over

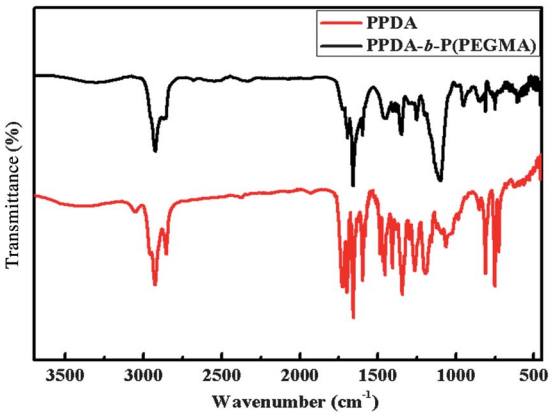

Fig. 3 FT-IR spectra: PPDA homopolymer (red curve) and PPDA-*b*-P(PEGMA) copolymer (black curve).

molecular weight distribution. Homogeneous nanoparticles can be formed through the self-assembly of uniform amphipathic copolymers in aqueous solution. As is known, the typical amphiphilic diblock polymer polystyrene-*block*-poly(acrylic acid) (PS-*b*-PAA) can self-assemble into micelles with a PS core and PAA shell in DMF–H_2O solution. The base-catalyzed sol–gel process inside the PS core induces the formation of PAA-encapsulated hybrid core–shell nanospheres.[32] As a uniform amphiphilic diblock copolymer, we predict that PPDA-*b*-P(PEGMA) should show self-assembly behavior in water. So, the PPDA-*b*-P(PEGMA) diblock copolymer was dispersed in water by ultrasonication and indeed conveniently formed nanoparticles. The route for preparing PNPs is shown clearly in Scheme 2. The photophysical, topographic properties of these homogeneous nanoparticles and their biocompatibility with cells were studied.

3.2. Nanoparticle morphology

To confirm that the PPDA-*b*-P(PEGMA) copolymers can self-assemble into nanoparticles in aqueous solution, their

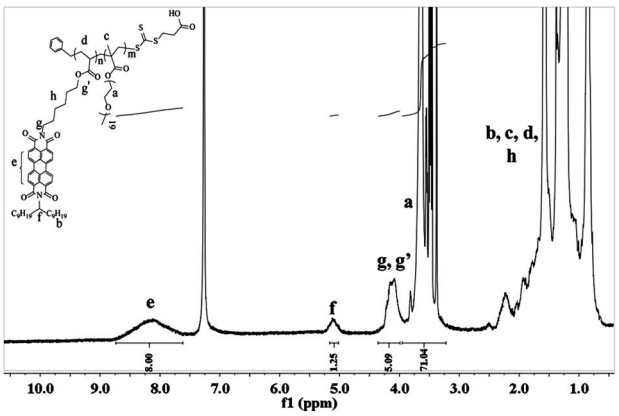

Fig. 2 The ^{1}H-NMR spectrum of the PPDA-*b*-P(PEGMA) copolymer in $CDCl_3$. The assignment of the aromatic protons is correlated to the labeled structure shown in the inset.

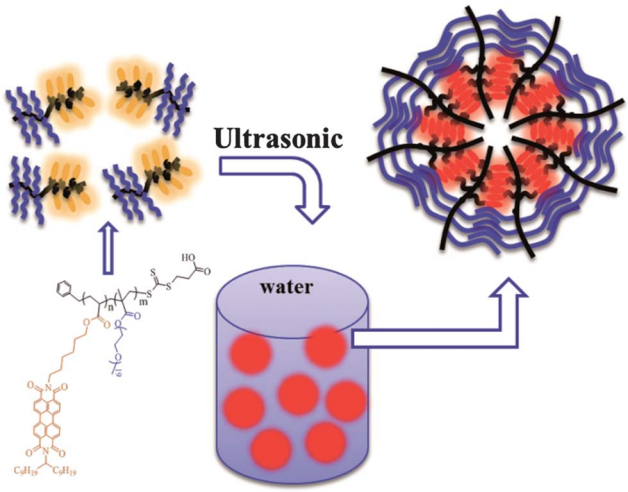

Scheme 2 Schematic of the preparation of PPDA-*b*-P(PEGMA) PNPs.

morphological properties were investigated. TEM was employed to study the morphology of solid films of the diblock copolymer, as shown in Fig. 4(a) and (b). Sufficient "phase contrast" is obtained by a proper amount of objective lens defocus in the bright-field mode of TEM. It can be seen that, upon evaporation of the water, the PPDA-*b*-P(PEGMA) copolymer forms a nanosphere morphology with a relatively constant diameter of about 50.0 ± 2.2 nm. SEM (Fig. 5) confirms the spherical structure with good dispersibility, and the size is consistent with the TEM observation. Dynamic light scattering (DLS) measurements were further carried out to determine the hydrodynamic particle size of the whole nanoparticle range. The DLS measurements revealed that all the PNPs have a relatively narrow size distribution with a mean size of around 64.3 ± 3.3 nm (Fig. 6) in aqueous solution. The size of the PNPs observed under TEM is smaller than the DLS result due to their shrinking in the dry state.

It is well established that NMR is an important tool for detecting the formation and structures of micelles in solutions of diblock copolymers.[33] Because of the insoluble nature of the components within the micelle core, their NMR signals generally cannot be observed. Fig. 7 presents the ^{1}H-NMR spectrum of a PPDA-*b*-P(PEGMA) copolymer in D_2O. Compared with the ^{1}H-NMR spectrum of this copolymer in $CDCl_3$, only the peaks at 3.52 ppm arising from the PEGMA segment can be observed in D_2O, and the peaks due to hydrogens on the aromatic rings and alkyl chains from the PDI groups at 8.2 ppm, 4.1 ppm and 1.4 ppm, respectively in $CDCl_3$ (Fig. 2) have totally disappeared in D_2O. This phenomenon strongly verifies that the hydrophobic PPDA chains were effectively encapsulated by the hydrophilic P(PEGMA) chains.

3.3. Optical properties characterization

To better understand the aggregation behavior of PDI groups in PPDA-*b*-P(PEGMA), we first studied the difference in optical properties between the PDA monomer and PPDA-*b*-P(PEGMA) at the same concentration (the concentration of PDI groups) in the good solvent $CHCl_3$. Thelakkat *et al.* reported that individual PDI molecule has two spectral features, the fingerprint bands of PDIs at 530 nm and the vibronic progression peaks of PDIs at 490 and 460 nm in solution. Once the strong π–π stacking among PDIs is formed, the intensities of the vibronic progression peaks at 490 nm and 460 nm will become higher than the fingerprint bands of PDIs at 530 nm.[34] Thus the intensity variation of the absorption peaks at 460, 490 and 530 nm of the PDI groups can be used to investigate their π–π stacking behavior. Fig. 8(a) shows the normalized absorption of PDA monomers and PPDA-*b*-P(PEGMA) dissolved at the same concentration (10 μM, the concentration of PDI groups) in $CHCl_3$. The PDA monomer exhibited the characteristic absorption properties of the individual PDI molecule, and the intensities of the fingerprint bands of PDIs at 530 nm is higher than the vibronic progression peaks at 490 and 460 nm. In the absorption of the PPDA-*b*-P(PEGMA) copolymer, the intensities of the vibronic progression peaks at 490 and 460 nm are obviously strengthened in comparison with that of the PDA monomer, indicating the enhanced π–π stacking in the copolymer than in the monomer. Furthermore, compared with the emission peaks at 530 and 570 nm of the PDA monomer in $CHCl_3$ (Fig. 8(a)), a new red emission peak at 620 nm of PPDA-*b*-P(PEGMA) appeared due to the formation of π–π stacking in the diblock copolymer. All the results demonstrated that it is easier for PPDA-*b*-P(PEGMA) to form π–π stacking than for the PDA monomer. Although PPDA-*b*-P(PEGMA) and PDI monomer can both be well dissolved in $CHCl_3$, the local concentration of PDI groups

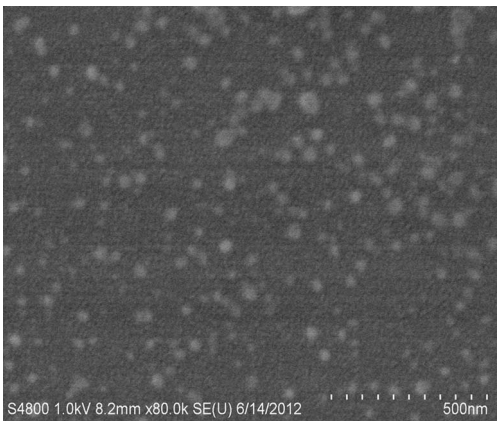

Fig. 5 SEM image of the self-assembled PNPs of PPDA-*b*-P(PEGMA).

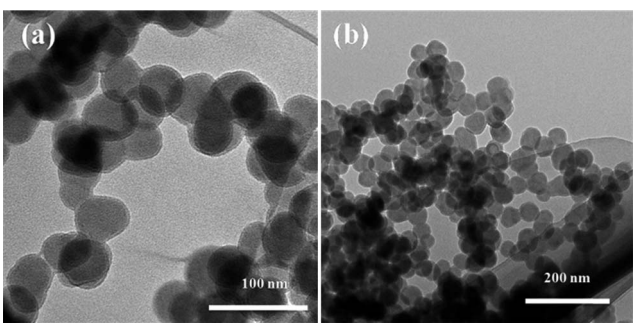

Fig. 4 TEM images of the self-assembled PNPs of PPDA-*b*-P(PEGMA).

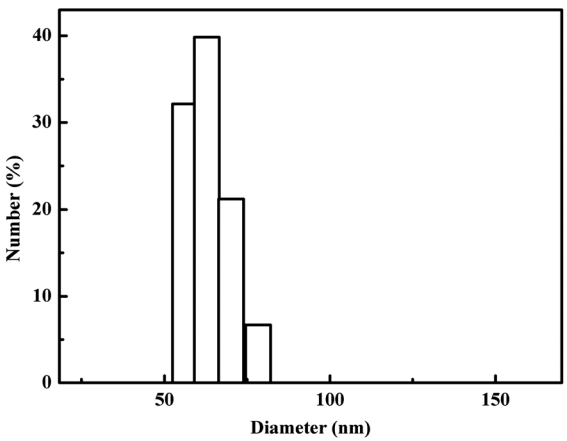

Fig. 6 Hydrodynamic size distribution graphs of the self-assembled PNPs of PPDA-*b*-P(PEGMA).

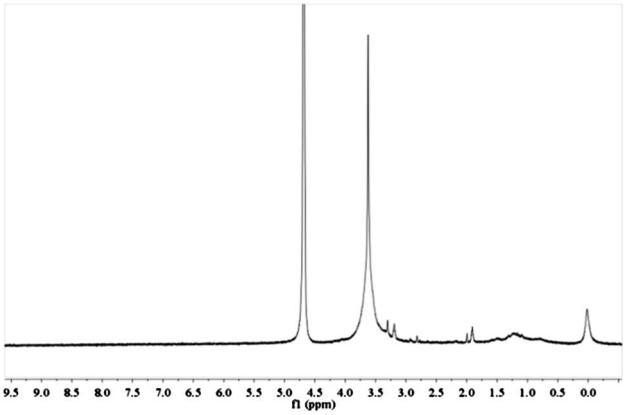

Fig. 7 The ^{1}H-NMR spectrum of the PPDA-*b*-P(PEGMA) copolymer in D_2O.

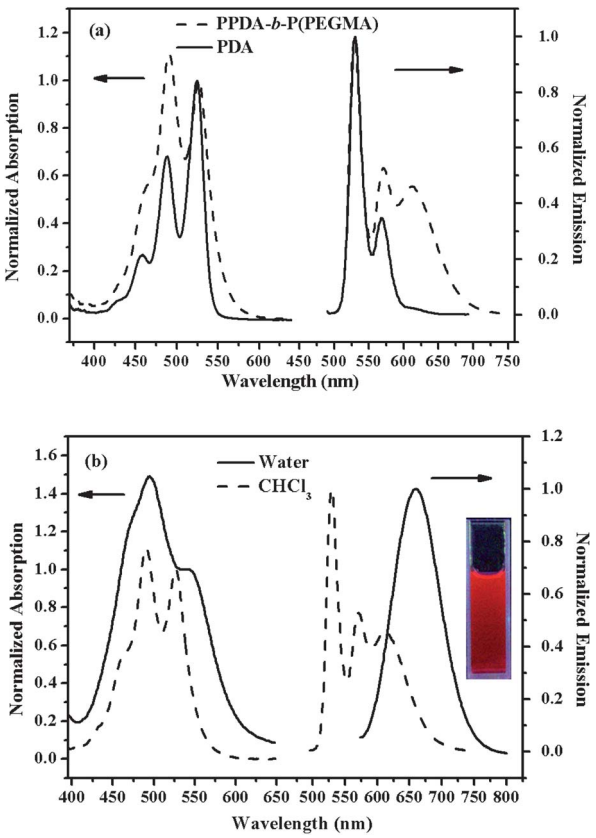

Fig. 8 (a) Normalized absorption and emission spectra of PDA monomers (solid line) and PPDA-*b*-P(PEGMA) (dashed line) dissolved at 10 μM concentration in $CHCl_3$. (b) Normalized absorption and emission of the PPDA-*b*-P(PEGMA) in water (solid line) and $CHCl_3$ (dashed line). The inset shows the PNPs in water exposed to 365 nm excitation using a portable fluorescent lamp.

in PPDA-*b*-P(PEGMA) is higher than that in PDA monomer because of the confined movement of those PDI groups which are chemically combined together on the PPDA chains. Consequently, the enhanced local concentration of PDI groups contributes to the formation of intrachain π–π stacking and red-shifted emission.

The aggregation behavior of PPDA-*b*-P(PEGMA) in aqueous solution was further studied, demonstrating the formation of more efficient π–π stacking than in $CHCl_3$. The UV-vis and PL spectra of PPDA-*b*-P(PEGMA) in aqueous solution and $CHCl_3$ solution are shown in Fig. 8(b). Comapred with PPDA-*b*-P(PEGMA) in $CHCl_3$, it is obvious that the intensities of the vibronic progression peaks of the PDI groups at 490 and 460 nm became much higher than the peak at 530 nm in water. Furthermore, the emission peaks at 530 nm and 570 nm in $CHCl_3$ solution disappeared entirely and only the NIR emission at 660 nm remained. All these observations indicated the stronger π–π stacking of the PDI groups formed in PPDA-*b*-P(PEGMA) aqueous solution. As discussed previously, the PNPs will form spontaneously through hydrophobic interactions after the amphiphilic diblock copolymers PPDA-*b*-P(PEGMA)s were dissolved in water. In PNPs, the hydrophobic PPDA chains aggregated together and dramatically enhanced the local concentration of PDI groups, and therefore promoted the efficient formation of interchain and intrachain π–π stacking and NIR emission, which is in agreement with the published report that the emission of PDIs can be red-shifted from 535 to 674 nm by enhanced π–π stacking.[22]

To further study the dependence of the optical properties of the polymer on the self-assembly behavior, the spectroscopic properties of this PPDA-*b*-P(PEGMA) polymer were investigated in aqueous solution by concentration-dependent UV-vis and fluorescence spectroscopy (Fig. 9). In Fig. 9, the absorption spectra feature the characteristic fingerprint bands with an absorption maximum at 460 nm, which indicates that there is strong π–π stacking among the PDIs as discussed above. There are almost no absorption changes observed over the whole range of copolymer concentrations from 0.0019 mg mL^{-1} to 0.3 mg mL^{-1}, which indicates that most of the aggregated PDI groups were present in water. The fluorescent behavior of the copolymer obviously showed that an increase in the polymer concentration resulted in higher NIR emission from the aggregated PDI groups, and conversely the emission peaks at 530 nm and 570 nm, which belong to the individual PDI groups, decreased gradually. When the concentration increased to 0.3

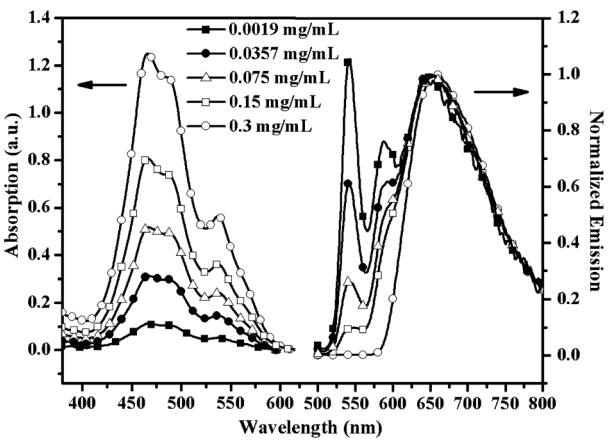

Fig. 9 UV-vis absorption and normalized PL emission spectra of PPDA-*b*-P(PEGMA) in water.

mg mL^{-1}, only the NIR emission at 660 nm remained, indicating that all the PDI groups were aggregated together. These results indicate that the polymer concentration highly influenced its optical properties in aqueous solution through self-assembly behaviors.

3.4. ^{1}H-NMR analysis

To further confirm that the π–π stacking of PDI groups is affected by its concentration, we studied the ^{1}H-NMR spectra at different concentrations of the PDA monomer in $CDCl_3$ (Fig. 10(a) and (b)). Its chemical shifts with varying concentrations ranging from 5, 10, 20, 30, 40 to 80 mg mL^{-1} can be obviously distinguished from the spectra. In the spectra shown in Fig. 10(a), as the concentration increased, the signals of the hydrogens on the aromatic ring of the PDI group were shifted upfield, but those of the hydrogens in other parts still remained at their original positions. This phenomenon is caused by the aromatic hydrogen suffering a shielding effect due to overlapping of the hydrogen orbitals and increased charge density from π–π stacking.[35] The remarkable red-shift in the fluorescence of the PDA monomers mentioned above (see inset photos in Fig. 10(a)) also supported that the π–π stacking increases with the increasing concentration of PDA monomers in $CDCl_3$.

The π–π stacking effect of the PDI groups in diblock copolymer PPDA-*b*-P(PEGMA) can also be evaluated from its ^{1}H-NMR spectrum. The ^{1}H-NMR spectrum (Fig. 2) of 10 mg mL^{-1} (6 mM, the concentration of the PDI group) PPDA-*b*-P(PEGMA) copolymer in $CDCl_3$ showed the chemical shifts of hydrogens on the aromatic rings of PPDA chains at 8.2 ppm. For the PDA monomer in Fig. 10(b), as the concentration increased from 5 to 80 mg mL^{-1} (6 to 100 mM, the concentration of the PDI group), the chemical shifts of the hydrogens on the aromatic rings of the PDA monomers gradually shifted from 8.6 to 8.2 ppm. Thus, compared with the concentration of the PDI group (100 mM) in the PDA monomer, the much lower concentration (6 mM) of the diblock copolymer needed to realize the same π–π stacking effect (the chemical shift of hydrogens on the aromatic rings of PDI group at 8.2 ppm) confirmed that it is much easier to realize π–π stacking in PDI groups as repeat units in a polymer than in the monomer. Although the ^{1}H-NMR signal of the PPDA chains cannot be obtained in aqueous solution, which makes it difficult to evaluate the π–π stacking of PPDA-*b*-P(PEGMA) nanoparticles in aqueous solution through ^{1}H-NMR signal variation of hydrogens on the PPDA chains, the disappearance of the ^{1}H-NMR signal of the PPDA chains in D_2O (Fig. 7) obviously demonstrated the existence of PPDA aggregation in PNPs. Information on their π–π stacking can be obtained from the optical properties of the PNPs in water, as we discussed in the optical properties characterization section.

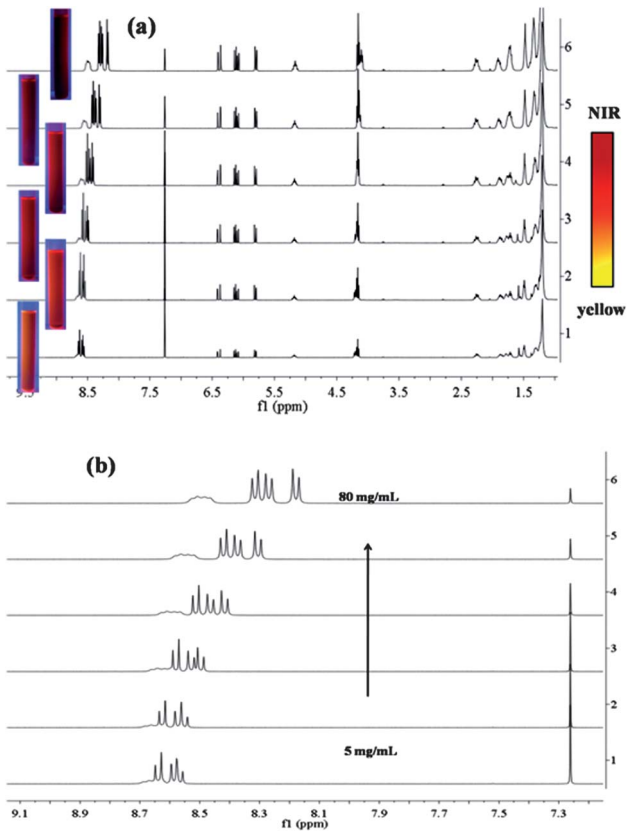

Fig. 10 (a) The full ^{1}H-NMR spectrum of the monomers in $CDCl_3$ and (b) the partial ^{1}H-NMR spectrum of the upfield shifting of the hydrogens on the aromatic ring of the monomers, corresponding to the different concentrations ranging from 5, 10, 20, 30, 40 to 80 mg mL^{-1} (from bottom to top). The inset shows the monomers with different concentrations in $CDCl_3$ exposed to 365 nm excitation by a portable fluorescent lamp.

3.5. Cytocompatibility properties and live cell imaging

To demonstrate the potential utility of the PNPs for cellular imaging, their cytocompatibility or cytotoxicity must be assessed. The cytocompatibility of the PNPs was evaluated in human pancreatic cancer cells (PANC-1) using an MTT cell viability assay. Fig. 11 summarizes the viability of the cells after being cultured with PNPs solutions at concentrations of 0.5, 0.1, 0.01, 0.001 and 0.0001 mg mL^{-1} for 24 h. These compounds showed relatively low cytotoxicity (over 85% viability) after 24 h

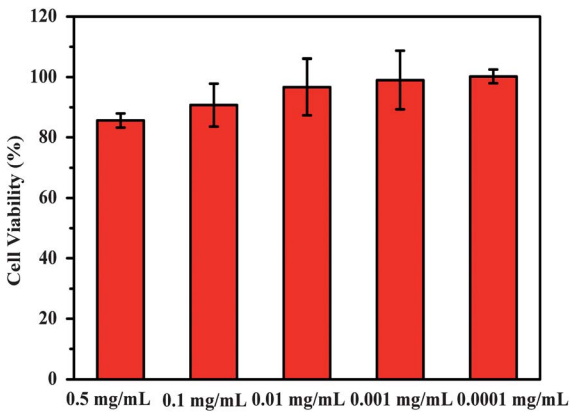

Fig. 11 *In vitro* viability of human pancreatic cancer cells (PANC-1) treated with different concentrations of PNPs solutions for 24 h.

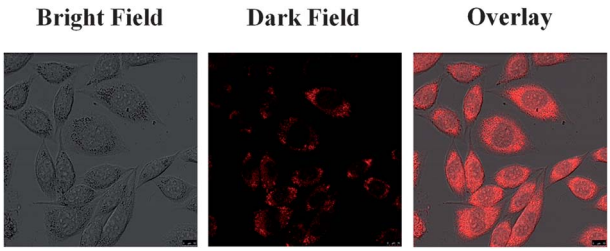

Fig. 12 Confocal microscopic images of PANC-1 cells after 24 h incubation with PNPs at 37 °C: (left) bright field image; (middle) overlay image; (right) dark field image. Scale bar = 0.1 mm.

of incubation time. This result indicates that the PEG encapsulation of perylene bisimides exhibited low cytotoxicity, which is attributed to the cytocompatibility of PEGMA.[36]

Live cell imaging based on the PNPs was investigated using confocal laser scanning microscopy (CLSM). Human pancreatic cancer cells (PANC-1) cells were tested to demonstrate the utility of the PNPs in cell imaging. After 24 h of incubation with the PNPs solution (0.01 mg mL^{-1}), the cells were washed three times in PBS buffer. The excitation wavelength was fixed at 530 nm. Fluorescent signals were collected from 550 nm to 750 nm. Fig. 12 shows the CLSM images of the PNPs-stained PANC-1 cells. Outstanding fluorescence from the cellular cytoplasm is observed for the PANC-1 cells. This result indicates that the PNPs were efficiently internalized by the PANC-1 cells and accumulated in the cytoplasm.

4. Conclusions

In summary, PDI functionalized with acrylate moieties was synthesized and then the amphiphilic diblock copolymers PPDA-*b*-P(PEGMA) were obtained *via* RAFT polymerization. PNPs with NIR emission were conviniently obtained through the direct self-assembly of the as-synthesized amphiphilic diblock polymer in water. This self-assembly contributed to PPDA aggregation through hydrophobic interactions and therefore enhanced the efficient π–π stacking of PDI groups to produce NIR emission. Furthermore, the PEGMA-encapsulation of the PNPs provided them with good water solubility and low cytotoxicity, which made these PNPs good candidates for live cell imaging. Our study demonstrated a convenient method to fabricate NIR-emitting PNPs with good water solubility and biocompatibilty through the self-assembly of amphiphilic diblock copolymers. It is anticipated that such a diblock copolymer-based amphiphilic structure built from controlled polymerization can be used to develop other aggregation-related optical probes, such as PNPs with aggregation-induced emission (AIE), aggregation-induced enhanced emission (AIEE), and so on.

Acknowledgements

This work was financially supported by the National Basic Research Program of China (no. 2009CB930600, 2012CB933301 and 2012CB723402), the Ministry of Education of China (no. IRT1148), the National Natural Science Foundation of China (no. 21222404, 51173080 and 21104033) and the Program for New Century Excellent Talents in University (no. NCET-10-0179), as well as the Specialized Research Fund for the Doctoral Program of Higher Education (no. 20093223110003) and the Natural Science Foundation of Jiangsu Province of China (no. BZ2010043, NY211003).

Notes and references

1 R. Weissleder, *Science*, 2006, **312**, 1168–1171.
2 C. Zhu, L. Liu, Q. Yang, F. Lv and S. Wang, *Chem. Rev.*, 2012, **112**, 4687–4735.
3 J. K. Jaiswal and S. M. Simon, *Nat. Chem. Biol.*, 2007, **3**, 92–98.
4 R. Weissleder, *Nat. Biotechnol.*, 2001, **19**, 316–317.
5 J. V. Frangioni, *Curr. Opin. Chem. Biol.*, 2003, **7**, 626–634.
6 L. Zhang and A. Eisenberg, *Science*, 1995, **268**, 1728–1731.
7 M. De, P. S. Ghosh and V. M. Rotello, *Adv. Mater.*, 2008, **20**, 4225–4241.
8 B. X. Gao, H. X. Li, H. M. Liu, L. C. Zhang, Q. Q. Bai and X. W. Ba, *Chem. Commun.*, 2011, **47**, 3894–3896.
9 D. T. McQuade, A. E. Pullen and T. M. Swager, *Chem. Rev.*, 2000, **100**, 2537–2574.
10 A. Kaeser and A. P. H. J. Schenning, *Adv. Mater.*, 2010, **22**, 2985–2997.
11 J. H. Kim, K. Park, N. Y. Nam, S. Lee, K. Kim and I. C. Kwon, *Prog. Polym. Sci.*, 2007, **32**, 1031–1053.
12 S. M. Lindner, S. Hüttner, A. Chiche, M. Thelakkat and G. Krausch, *Angew. Chem., Int. Ed.*, 2006, **45**, 3364–3368.
13 Y. Liu, K. Wang, D. S. Guo and B. P. Jiang, *Adv. Funct. Mater.*, 2009, **19**, 2230–2235.
14 T. Ohta, T. Nagano, K. Ochi and Y. Kubozono, *Appl. Phys. Lett.*, 2006, **89**, 053508.
15 P. P. Neelakandan, Z. Pan, M. Hariharan, Y. Zheng, H. Weissman, B. Rybtchinski and F. D. Lewis, *J. Am. Chem. Soc.*, 2010, **132**, 15808–15813.
16 B. Wang and C. Yu, *Angew. Chem., Int. Ed.*, 2010, **49**, 1485–1488.
17 F. J. Cespedes-Guirao, A. B. Ropero, E. Font-Sanchis, A. Nadal, F. Fernandez-Lazaro and A. Sastre-Santos, *Chem. Commun.*, 2011, **47**, 8307–8309.
18 H. Kobayashi, M. Ogawa, R. Alford, P. L. Choyke and U. Yasuteru, *Chem. Rev.*, 2010, **110**, 2620–2640.
19 L. Wang, L. Xu, K. G. Neoh and E. T. Kang, *J. Mater. Chem.*, 2011, **21**, 6502–6505.
20 D. Gorl, X. Zhang and F. Würthner, *Angew. Chem., Int. Ed.*, 2012, **51**, 6328–6348.
21 T. L. Andrew and T. M. Swager, *Macromolecules*, 2011, **44**, 2276–2281.
22 W. Wang, J. J. Han, L. Q. Wang, L. S. Li, W. J. Shaw and A. D. Q. Li, *Nano Lett.*, 2003, **3**, 455–458.
23 M. Sommer, S. M. Lindner and M. Thelakkat, *Adv. Funct. Mater.*, 2007, **17**, 1493–1500.
24 G. Moad, E. Rizzardo and S. H. Thang, *Polymer*, 2008, **49**, 1079–1131.

25 K. Knop, R. Hoogenboom, D. Fischer and U. S. Schubert, *Angew. Chem., Int. Ed.*, 2010, **49**, 6288–6308.
26 D. Lensen, D. M. Vriezema and J. C. M. van. Hest, *Macromol. Biosci.*, 2008, **8**, 991–1005.
27 Z. Liu, K. Chen, C. Davis, S. Sherlock, Q. Cao, X. Y. Chen and H. J. Dai, *Cancer Res.*, 2008, **68**, 6652–6660.
28 S. Rajaram, P. B. Armstrong, B. J. Kim and J. M. Fréchet, *Chem. Mater.*, 2009, **21**, 1775–1777.
29 S. M. H. Tenzel, T. P. Davis and A. G. Fane, *J. Mater. Chem.*, 2003, **13**, 2090–2097.
30 Q. Zhang, A. Cirpan, T. P. Russell and T. Emrick, *Macromolecules*, 2009, **42**, 1080–1082.
31 M. M. Ali and H. D. H. Stover, *Macromolecules*, 2004, **37**, 5219–5227.
32 D. Hvasanov, J. Wiedenmann, F. Braet and P. Thordarson, *Chem. Commun.*, 2011, **47**, 6314–6316.
33 S. Lu, Q. L. Fan, S. Y. Liu and S. J. Chua, *Macromolecules*, 2002, **35**, 9875–9881.
34 F. Spreitler, M. Sommer, M. Thelakkat and J. Köhler, *Phys. Chem. Chem. Phys.*, 2012, **14**, 7971–7980.
35 A. S. Shetty, J. S. Zhang and J. S. Moore, *J. Am. Chem. Soc.*, 1996, **118**, 1019–1027.
36 H. M. Liu, Y. L. Wang, C. H. Liu, H. X. Li, B. X. Gao, L. C. Zhang, F. L. Bo, Q. Q. Bai and X. W. Ba, *J. Mater. Chem.*, 2012, **22**, 6176–6181.